UDK 669.058.6:691.714:621.791.725
Original scientific article/Izvirni znanstveni članek

ISSN 1580-2949
Mater. Tehnol.

STUDY ON THE DYNAMIC COMPRESSION PROPERTIES OF A 0.5 % GRAPHENE/6061 ALUMINUM MATRIX COMPOSITE

ŠTUDIJ LASTNOSTI KOVINSKEGA KOMPOZITA NA OSNOVI ZLITINE VRSTE Al6061, OJAČANE Z 0,5 % GRAFENA ZARADI DINAMIČNIH TLAČNIH OBREMENITEV

Qinghui Song, Xiaoming Du*, Weiye Dong, Haicheng Liang, Hongwei Shi, Junze Liu

School of Materials Science and Engineering, Shenyang Ligong University, Shenyang 110159, China

Prejem rokopisa – received: 2025-03-27; sprejem za objavo – accepted for publication: 2025-10-07

doi:10.17222/mit.2025.1428

Dynamic compression experiments were conducted on a 0.5 *w*/% graphene/6061 aluminum matrix composite using a split Hopkinson pressure bar (SHPB) at varying strain rates. The effects of these strain rates on the mechanical properties and deformation damage of the graphene/6061 aluminum matrix composite were analyzed. The results indicate that the composite exhibits significant strain rate sensitivity; specifically, the yield strength of the composite progressively increases with the rise in compressive strain rate, and high strain rate compression leads to notable grain refinement. Additionally, the finite element method was utilized to establish a corresponding numerical model to simulate impact compression at high strain rates. It was observed that the primary internal damage during the compression process is interface damage. When compared to the experimental results, the trends in mechanical changes are similar, and the error falls within a reasonable range, thereby validating the effectiveness of the finite element simulation.

Keywords: aluminum matrix composite, graphene, dynamic compression, strain rate sensitivity

V članku avtorji opisujejo preizkuse dinamičnega obremenjevanja (utrujanja) kompozita z osnovo iz Al zlitine tipa Al6061 ojačane z 0,5 *w*/% grafena. Preizkuse so izvajali pri različnih hitrostih defornacije na tako imenovani napravi z deljenim Hopkinsovim tlačnim preizkušancem (SHPB; angl.: Split Hopkinson Pressure Bar). Avtorji so nato analizirali vpliv hitrosti deformacije na mehanske lastnosti in deformacijske poškodbe izbranega kompozita. Rezultati so pokazali, da je preizkušani kompozit zelo občutljiv na hitrost deformacije; še posebej meja plastičnosti kompozita postopoma narašča s hitrostjo tlačne deformacije in velika hitrost tlačne deformacije prispeva bistveno k udrobljenju (zmanjšanju velikosti) kristalnih zrn kovinske matrice kompozita. S pomočjo izdelanega numeričnega modela na osnovi metode končnih elementov (FEM; Finite Element Method) so avtorji simulirali udarno tlačno deformacijo pri visokih hitrostih deformacije. Opazili so, da primarna notranja poškodba materiala med procesom tlačenja nastaja na mejnih ploskvah med kristalnimi zrni kovinske matrice in ojačitveno fazo. Ko so primerjali eksperimentalne rezultate s simulacijami so opazili podobne trende pri mehanskih spremembah in razlike med njimi so bile v sprejemljivem območju napak. Tako so avtorji ovrednotili in potrdili tudi učinkovitost izdelanega modela ter izvedenih FEM simulacij.

Ključne besede: kompoziti na osnovi matrice iz aluminijeve zlitine, grafen, dinamične tlačne obremenitve, občutljivost na hitrost deformacije

1 INTRODUCTION

In recent years, aluminum matrix composites have gained widespread application in aerospace, military, and industrial fields due to their exceptional mechanical and physical properties. The mechanical characteristics of aluminum alloys can be significantly enhanced by incorporating reinforcement phases such as graphene, Al_2O_3, SiC and other phases. Among these, graphene stands out for its high mechanical stiffness and strength, demonstrating remarkable potential as a reinforcement phase in various composite materials.[1–6] In practical engineering applications, materials are often subjected to dynamic impact loads. Therefore, studying the dynamic mechanical properties of composite materials is essential, as they directly affect the service life of the material components.

Many researchers have investigated the dynamic compression properties of particle-reinforced aluminum matrix composites. Fu et al.[7] utilized a split Hopkinson pressure bar apparatus to perform high strain rate compression experiments on SiCp/Al matrix composites with varying particle contents at different strain rates. The results indicated that SiCp enhanced the strain rate sensitivity of the composites, which increased with the rising strain rate. Alteneiji et al.[8] performed dynamic compression experiments on ceramic/aluminum composites and found that both the yield strength and dynamic Young's modulus of the composites increased with the strain rate. Notably, the strain rate sensitivity became significant when the strain rate exceeded 1000 s^{-1}. Zaiemyekeh et al.[9] examined the quasi-static and dynamic behavior of

*Corresponding author's e-mail:
du511@163.com (Xiaoming Du)

© 2025 The Author(s). Except when otherwise noted, articles in this journal are published under the terms and conditions of the Creative Commons Attribution 4.0 International License (CC BY 4.0).

aluminum composites reinforced with varying Al_2O_3 mass fractions, indicating that the addition of 5.0 *w*/% Al_2O_3 substantially improved the compressive strength and energy absorption capacity of the aluminum composites.

Due to its ultra-high elastic modulus, mechanical strength, and excellent thermal conductivity, graphene has garnered significant attention from researchers. It has been incorporated into aluminum matrix composites as a reinforcing phase, leading to substantial improvements in the mechanical properties of graphene/aluminum composites. Kumar et al.[10] investigated the tensile mechanical properties and microstructure of multilayer graphene aluminum matrix composites. Their results indicated that the mechanical properties of composites with a uniform distribution of graphene were significantly enhanced compared to those without a reinforcing phase. Rashad et al.[11] examined the effect of graphene nanosheets on the tensile, compressive, and hardness properties of aluminum matrix composites. They found that the tensile strength, compressive strength, and hardness of the Al-0.3 *w*/% graphene nanosheet composite increased by (11.1, 7.8, and 11.8) %, respectively, compared to pure aluminum. Currently, most research on graphene/aluminum composites is concentrated on tensile and static compression properties, while studies on dynamic impact compression loads are relatively scarce, with only a few investigations reporting on their dynamic compression characteristics. Zhao et al.[12] reported on the dynamic mechanical behavior of graphene nanoflake-reinforced aluminum matrix composites. Their results showed that aluminum matrix composites are high strain rate-sensitive materials.

In recent years, numerous researchers have employed finite element methods to investigate and predict the properties of aluminum matrix composites, particularly the mechanical properties of graphene/Al composites. Dahiya et al.[13–15] developed a three-dimensional finite element volume element capable of predicting the mechanical properties of nanographene-reinforced aluminum composites. They examined the effects of varying mass fractions, graphene sizes, and orientations on the tensile mechanical properties of these composites. Additionally, they utilized a similar nanographene-reinforced aluminum composite model to analyze the effect of different graphene sizes and distribution states on the elastic modulus, yield strength, and tensile strength. Su et al.[16] created a three-dimensional structural model of graphene/Al composites using a self-developed structural modeling program, focusing on the interface behavior and fracture failure characteristics of the model.

In this paper, a 0.5 *w*/% graphene/aluminum matrix composite was prepared using the powder metallurgy method. Dynamic impact compression experiments were conducted using a SHPB to investigate the dynamic mechanical properties of the composite at various strain rates. Additionally, a corresponding finite element model was established to predict the dynamic mechanical response of the composite at different strain rates. The numerical model was validated against the experimental results based on the stress-strain relationship.

2 EXPERIMENTAL DETAILS

2.1 Materials

The composite included high-purity 6061 aluminum powder (purity ≥ 99 %) with a particle size of 10 μm (Beijing Hongyu Materials Co., Ltd.) as the matrix. The reinforcing phase consisted of graphene with a size range of 5–10 μm and a thickness of 3–5 nm (Jiangsu Xianfeng Nanomaterials Technology Co., Ltd.). A mass fraction of 0.5 *w*/% graphene was mixed with the aluminum powder in a 5:1 pellet ratio using a mixer at 300 min^{-1} for 6 h. The mixed powder was then placed in a mold and sintered in a vacuum hot-pressing furnace at 610 °C and 50 MPa. Subsequently, the sintered composite underwent solid solution treatment at 450 °C for 2 h, followed by aging treatment at 160 °C for 16 h. This process aimed to enhance the performance of the graphene/6061 aluminum matrix composite.

2.2 Compression testing

The dynamic mechanical properties of the graphene/6061 aluminum matrix composite were investigated at room temperature. SHPB experiments were conducted on the samples at various strain rates (2000 s^{-1}, 3000 s^{-1}, and 4500 s^{-1}) to minimize errors caused by inertia effects.[17] The specimens were machined to a diameter of 7 mm and a length of 5 mm. A quasi-static compression test (strain rate of 10^{-3} s^{-1}) was performed using samples of the same dimensions. A Hitachi S-3400 scanning electron microscope (SEM) and a 200TAM metallographic microscope were employed to examine the microstructure of the samples before and after compression.

3 MODELS AND METHODS

3.1 Material parameters

Graphene is regarded as a linear elastic and isotropic material. The Johnson-Cook model was employed for both the matrix material of 6061 aluminum alloy and the graphene-reinforced phase, as it effectively describes the plastic deformation behavior of a material under varying strain rates. This model is frequently utilized to characterize the mechanical response of materials under different deformation conditions.[18,19] The core components of the model account for the strain hardening effect, strain rate effect, and temperature softening effect of the material.[20] The model employs a multiplicative relationship to address the influence of these three factors on the dynamic yield stress. Since this experiment was conducted at room temperature without considering the temperature

Table 1: Material parameters for aluminum and graphene

Material	Density (g/cm^3)	Elastic modulus (GPa)	Poisson's ratio	*A* (MPa)	*B* (MPa)	*n*	*C*
6061Al[22]	2.7	71	0.3	278.2	245.2	0.817	0.0256
Graphene[23]	1.5	1100	0.17	354.3	1549.9	0.684	0.0368

softening effect, the expression of the Johnson-Cook model is as follows:[21]

$$\sigma = (A + B\varepsilon^{n})1 + C \ln \frac{\dot{\varepsilon}}{\dot{\varepsilon}_0}$$

where *A*, *B*, *C*, and *n* represent the yield stress, strain hardening coefficient, strain rate hardening parameter, and material hardening index of the material under quasi-static conditions, respectively. Additionally, $\dot{\varepsilon}$ and $\dot{\varepsilon}_0$ denote the strain rate and reference strain rate, respectively. Specific material parameters are presented in **Table 1**.

3.2 Finite element model

A 0.5 *w*/% graphene/6061 aluminum matrix composite Representative Volume Element (RVE) model was constructed using the finite element (FE) module in DIGIMAT software. The influence of the reinforcement phase shape on the mechanical properties and damage of the composite was examined in conjunction with existing literature.[24] In the model, graphene is represented as randomly distributed circular discs with a diameter-to-thickness ratio of 20:1. A total of six discs are included to achieve the graphene mass fraction of 0.5 %. It is assumed that graphene is multi-layered. The model is shown in **Figure 1a**. The generated RVE model was imported into a finite element program, where dynamic compression simulations were conducted using the explicit dynamic analysis method. The model was discretized with 3D quadratic tetrahedral elements, resulting in a total of 25815 elements. Due to the complex structure of the SHPB experimental device, only the composite material model was simulated to facilitate modeling and simplify calculations. The fixed and dynamic compression loading of the model was achieved through displacement control under specified boundary conditions, with different strain rates obtained by varying the loading displacements and durations. The constraint and loading model is illustrated in **Figure 1b**.

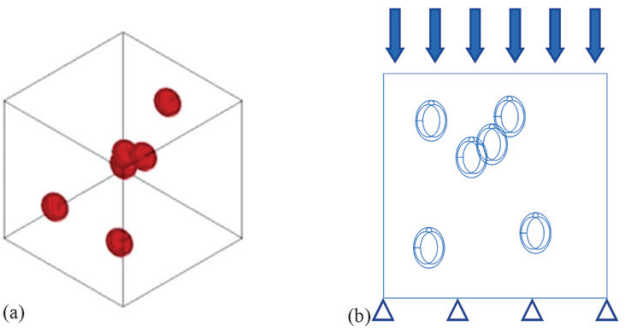

Figure 1: Numerical finite element model of the 0.5 *w*/% graphene/6061 aluminum matrix composite: a) three-dimensional model, b) constraint and loading model

4 RESULTS AND DISCUSSION

4.1 Dynamic compression performance

Figure 2 illustrates the stress-strain curves of the graphene-reinforced 6061 aluminum matrix composite subjected to compression at various strain rates. The composite remains in the elastic deformation stage when the strain is below 0.05, during which the flow stress increases rapidly with strain. Subsequently, the composite transitions into the plastic deformation stage, where the flow stress changes more gradually as the strain increases. Under quasi-static loading conditions, the yield strength of the material is 283 MPa. In contrast, under dynamic loading conditions, the yield strength of the composite increases with the strain rate. At strain rates of (2000, 3000, and 4500) s^{-1}, the yield strengths are (357.5, 366.81 and 375.05) MPa, respectively. These values represent increases of (26.3, 29.6, and 32.5) %, respectively, highlighting the influence of the strain rate hardening on the properties of the composite.

When the composite is subjected to dynamic loading, internal stress is transferred from the low-strength aluminum to the high-performance graphene through the interface between aluminum and graphene. This transfer allows graphene to share part of the load with the aluminum matrix, thereby enhancing the load-bearing

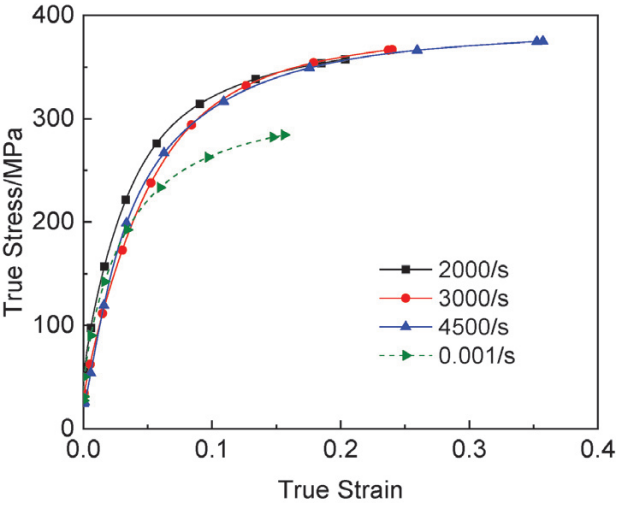

Figure 2: Stress-strain curves of the graphene/6061 Al composite at various strain rates

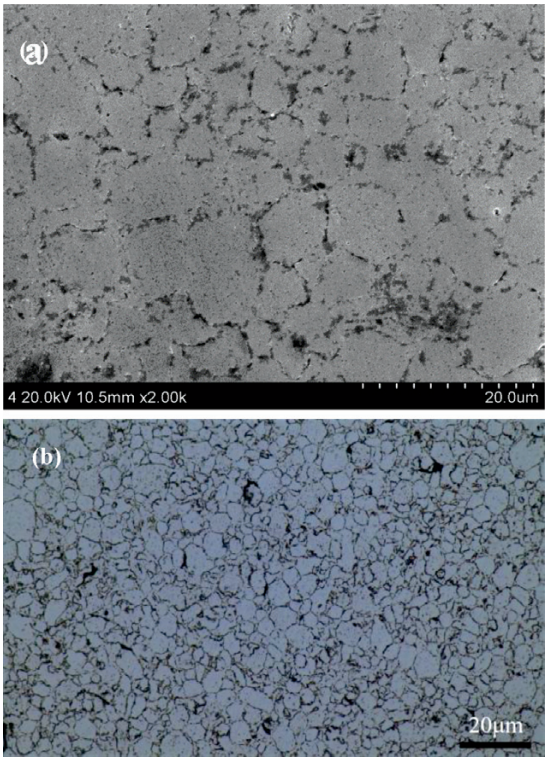

Figure 3: Microstructure image of the 0.5 *w*/% graphene/6061 aluminum matrix composite before the experiment: a) SEM image; b) metallographic microscopic image

capacity of the composite material. Under impact loading, the aluminum matrix grains initially slip and deform. Simultaneously, the uniform distribution of the second-phase particles, graphene, obstructs the dislocation movement of the matrix grains and causes them to distort around the graphene. This interaction enhances the compressive properties of the composite and exhibits strain hardening. The thermal expansion coefficients of graphite and aluminum are 10^{-6} K^{-1} and 23.6×10^{-6} K^{-1}, respectively. This significant difference leads to the formation of dislocations at the interface of the graphene-aluminum composite during prismatic punching, which enhances the strength of the composite matrix. The density of dislocations is influenced by the surface area of the reinforcing particles; smaller particles result in a higher dislocation density, thereby increasing the strength of the composite.[25] Since the added graphene reinforcement consists of nanoscale particles, a dislocation ring forms around each reinforcing phase.[26] This ring hinders the migration of dislocations, further increasing the yield stress of the composite.

From the dynamic compressive stress-strain curve, it can be observed that once the material enters the plastic deformation stage, the change in flow stress gradually decreases, particularly at a strain rate of 4500 s^{-1}. This phenomenon occurs because, at room temperature, the dynamic compression of composite materials at high strain rates resembles an adiabatic compression process, generating a significant amount of heat within the material. There is insufficient time for this heat to dissipate, leading to an increase in temperature that softens the material and reduces its load-bearing capacity. Fiedler et al.[27] investigated the compression process of aluminum matrix composites at high loading speeds using infrared thermal imaging equipment. They found that significant temperature changes occurred during compression, with concentrated plastic deformation occurring in the regions where the temperature increased.

As the strain rate increased, the strain range of the material also expanded. When the strain rate increased from 2000 s^{-1} to 4500 s^{-1}, the maximum strain value rose from 0.2 to 0.36. Meanwhile, the energy absorption of the composite during compression was determined by calculating the area under the stress-strain curve following impact compression (W).[28] It was found that the energy absorption capacity of the composite increases with the strain rate, with maximum energy absorption capacities of (59.5, 69.9, and 113.2) MJ/m^3 at strain rates of (2000, 3000, and 4500) s^{-1}, respectively.

4.2 Microstructure following dynamic compression

Figure 3 presents a SEM image and a metallographic microscopic image of the 0.5 *w*/% graphene/6061 aluminum matrix composite prior to the impact experiment. The figure shows that the majority of graphene is uniformly distributed along the grain boundaries of the aluminum matrix, with only a small portion located on the grains of the aluminum matrix. Notably, the SEM image reveals no signs of graphene agglomeration. The bonding

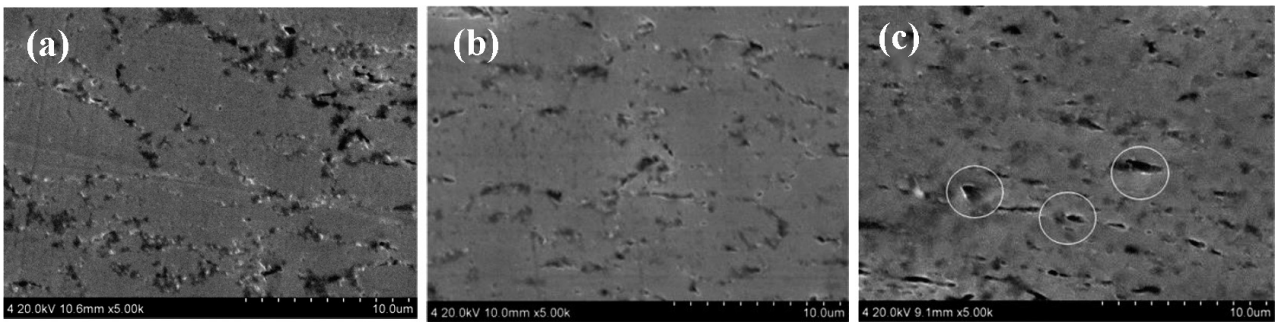

Figure 4: SEM images of the 0.5 *w*/% graphene/6061 aluminum composite after dynamic compression at various strain rates: a) 2000 s^{-1}; b) 3000 s^{-1}; c) 4500 s^{-1}

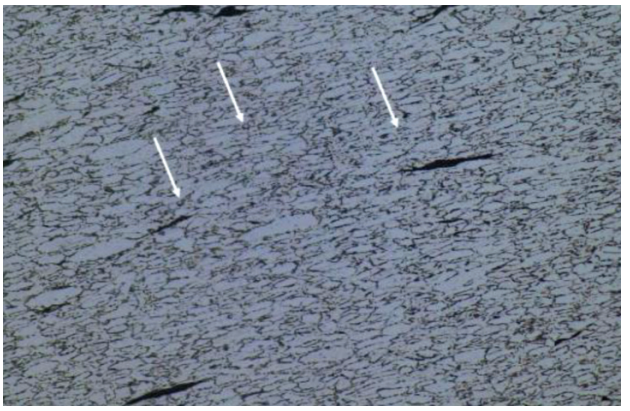

Figure 5: Metallographic microscopic image of the 0.5 *w*/% graphene/6061 Al composite at a strain rate of 2000 s^{-1}

between the aluminum matrix and graphene is robust, with no micro-cracks observed and no evidence of graphene shedding.

Figures 4 and **5** show microstructural images of the composite subjected to dynamic compression at varying strain rates. Compared to the pre-compression state, the grain size diminishes along the loading direction. Concurrently, as the strain rate increases, the grain boundaries between the grains gradually become less distinct. When the strain rate reaches 4500 s^{-1}, the grain boundaries become difficult to identify, and a few micropores (located within the area framed in white) are present, with the pore structure exhibiting a smooth surface. This phenomenon is attributed to the softening or melting of the sample at elevated temperatures. As noted above, the composite material remains in the adiabatic state during the dynamic compression process, which leads to an increase in the material temperature and a corresponding rise in dislocation density within the matrix. These two factors contribute to dynamic recrystallization within the material. This phenomenon is evidenced by the fine grains of various shapes located in the area indicated by the white arrow in **Figure 5**, with these grains predominantly found at the grain boundaries. As the strain rate increases, the deformation generated by the material within the same time frame also increases, resulting in greater heat accumulation. This enhanced heat facilitates more complete dynamic recrystallization, leading to finer recrystallized grains. Furthermore, a higher strain rate results in a greater dislocation density within the sample, which produces more dislocation cells and recrystallized structures, ultimately resulting in even finer recrystallized grains.

Figure 6 illustrates the macromorphology of the sample following dynamic compression. The deformation of the 0.5 *w*/% graphene/aluminum composite increases with the strain rate. At strain rates of 2000 s^{-1} and 3000 s^{-1}, the material structure remains intact, and no damage occurs, indicating that the composite material exhibits good plasticity below 3000 s^{-1}. However, when the strain rate is increased to 4500 s^{-1}, the central part of the sample remains intact, while grid-like cross cracks appear at the edges. **Figure 6b** presents a SEM image of the crack fracture in the composite material, which lacks ductile fracture characteristics such as tearing edges and dimpling. The structure of the fracture is smooth, with some areas exhibiting crystalline features, indicative of brittle fracture, and the fracture mode is classified as cleavage fracture.

4.4 Dynamic compression deformation damage

The equivalent stress distribution derived from the numerical simulation for the 6061 aluminum matrix and graphene at different strain rates is shown in **Figures 7** and **8**, respectively. The load is applied to the composite material in the direction indicated by the arrow. As shown in **Figure 7**, damage and failure primarily occur in the direction parallel to the impact velocity and are predominantly concentrated around the graphene. The incorporation of graphene significantly alters the stress distribution within the aluminum matrix. The area highlighted by the red arrow represents a locally enlarged view within the red box. Additionally, the stress cloud image on the graphene clearly illustrates the stress transfer occurring between the graphene and the matrix.

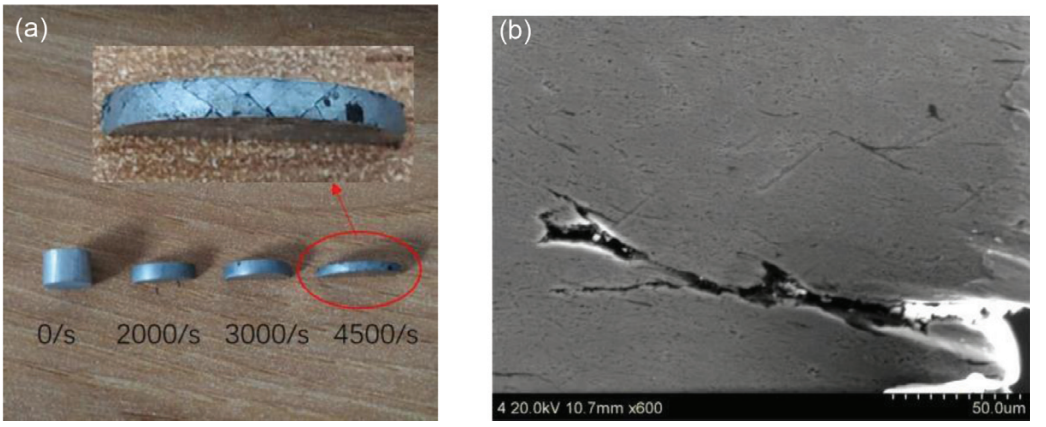

Figure 6: Macroscopic deformation and a SEM image of the 0.5 *w*/% graphene/6061 Al composite after dynamic compression: a) macroscopic deformation; b) SEM image

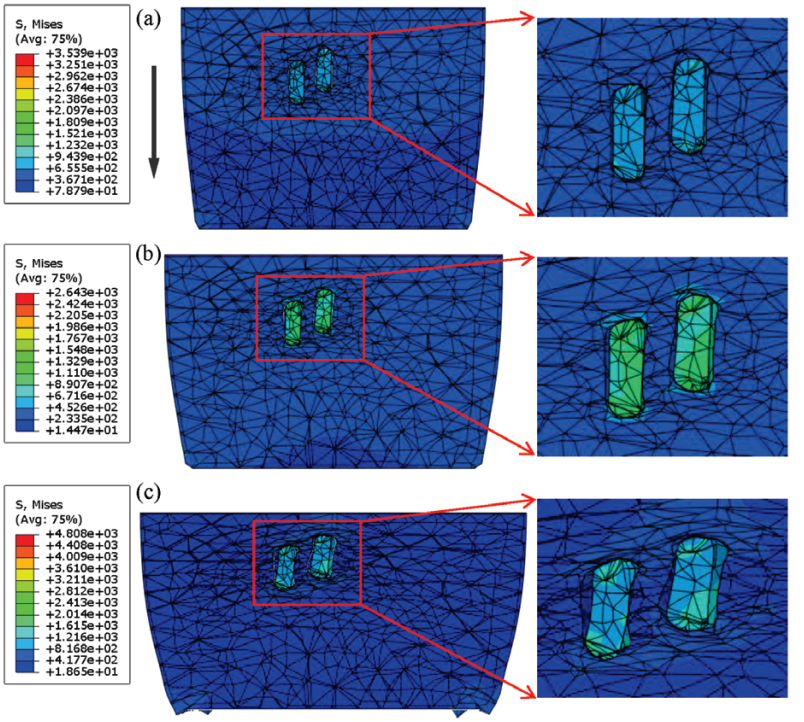

Figure 7: Equivalent stress distribution of the composite with a 0.5 *w*/% graphene content at various strain rates: a) 2000 s^{-1}; b) 3000 s^{-1}; c) 4500 s^{-1}

Moreover, the graphene dispersed within the aluminum matrix impedes the movement of the surrounding matrix, resulting in significant and dense deformation of the surrounding grid under load impact. Notably, the stress value of the surrounding matrix and the density of the grid increase with the strain rate. As illustrated in **Figure 8**, graphene particles exhibit pronounced stress concentration during the impact compression process. In this

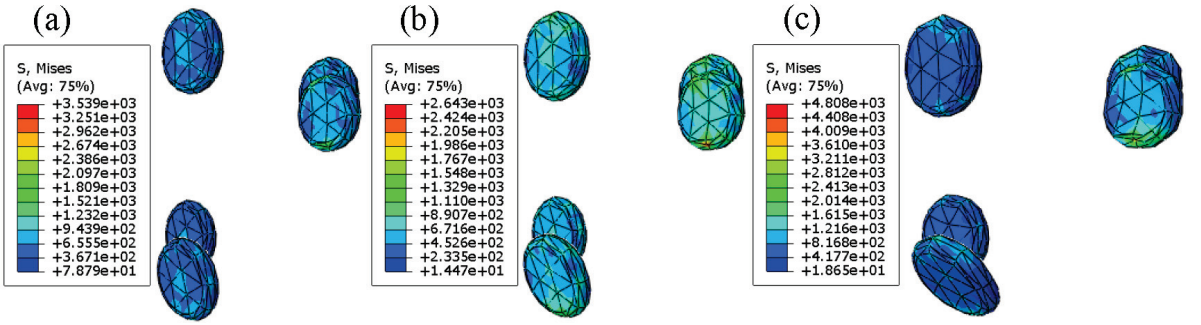

Figure 8: Distribution of equivalent stress in graphene particles at various strain rates: a) 2000 s^{-1}; b) 3000 s^{-1}; c) 4500 s^{-1}

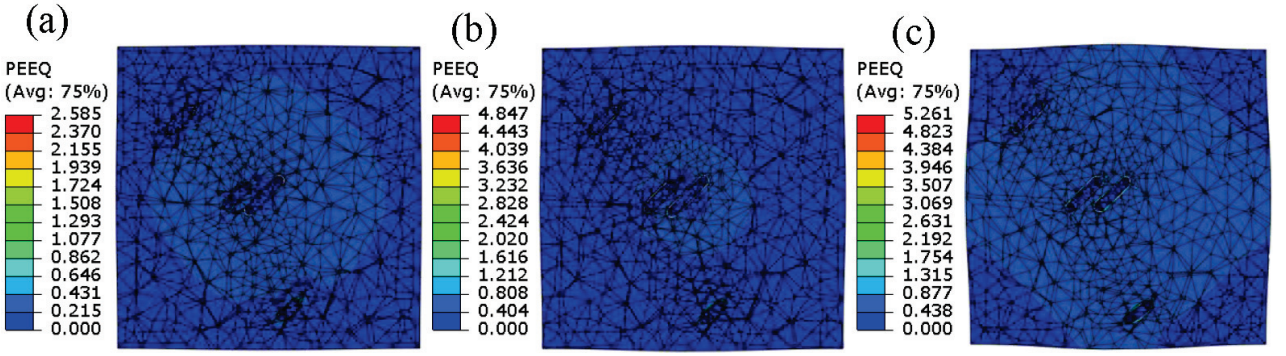

Figure 9: Equivalent strain distribution of the composite with a 0.5 *w*/% graphene content at various strain rates: a) 2000 s^{-1}; b) 3000 s^{-1}; c) 4500 s^{-1}

model, the matrix and the reinforcing phase are perfectly interfaced, without accounting for a third-phase material. Consequently, the stress on the graphene is directly transmitted to the aluminum matrix through the interface, and the strength of graphene is considerably greater than that of aluminum. When the load on the graphene accumulates to a certain threshold, the stress on the graphene decreases, leading to damage in the matrix.

It can be observed from **Figures 7a** to **7c** that the interface equivalent stress between the reinforcement phase and the matrix of the composite containing 0.5 *w*/% graphene is (367, 452, and 487) MPa, respectively. As the strain rate increases, the region of high stress at the interface expands. Additionally, as illustrated in **Figure 9**, with the same graphene content, the plastic deformation of the composite increases with the strain rate. Specifically, when the strain rate rises from 2000 s^{-1} to 4500 s^{-1}, the strain of the composite with 0.5 *w*/% graphene increases by 48 %. This indicates that the matrix in the interface region experiences significant plastic deformation, which may lead to detachment from the undeformed graphene and result in interface damage.

4.5 Comparison between numerical simulation and experimental results

The stress-strain curve of the graphene/6061 aluminum composite was simulated using a finite element model, as illustrated in **Figure 10**. It demonstrates that the numerical simulation results closely align with the experimental findings. The model accurately predicted the trend of change and the yield strength of the graphene/aluminum composite material, with an error margin of 10 %. However, a notable drawback is that the simulation results for the elastic stage of the finite element model significantly differ from the experimental results. This discrepancy arises from variations in loading stability, friction, and temperature during the experiment,

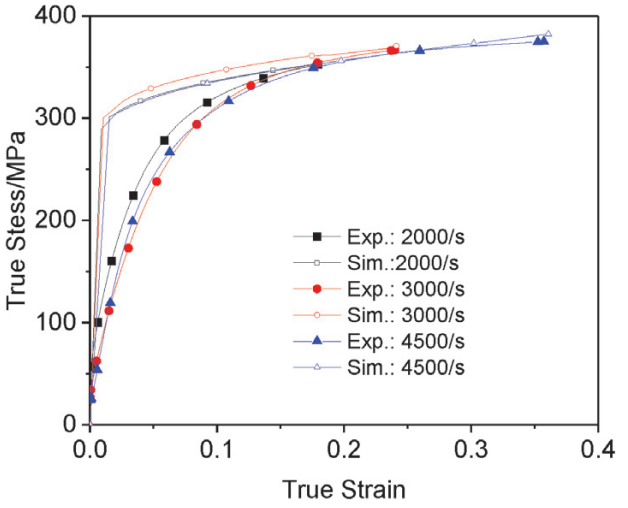

Figure 10: Comparison of stress-strain curves obtained from experimental and numerical simulations at various strain rates

which deviate from the ideal conditions assumed in the finite element model. Nevertheless, finite element analysis remains a convenient and efficient tool for analyzing and predicting the mechanical properties of graphene/aluminum composites under various loading conditions.

5 CONCLUSIONS

In this paper, a 0.5 *w*/% graphene/6061 aluminum matrix composite with a uniform distribution was prepared using the hot pressing sintering method. Compression experiments were conducted using a SHPB and a universal testing machine. Corresponding finite element models were developed using the finite element method to simulate impact compression at various strain rates. The effects of compression at different strain rates on the dynamic mechanical properties and deformation damage of the graphene/aluminum composite were investigated, leading to the following conclusions:

(1) The 0.5 *w*/% graphene/aluminum composite exhibited a significant strain rate strengthening effect. Compared to the quasi-static yield strength of 283 MPa, the yield strengths at strain rates of (2000 s^{-1}, 3000 s^{-1} and 4500 s^{-1} increased by (26.3, 29.6, and 32.5) %, respectively. However, at the strain rate of 4500 s^{-1}, the composite displayed noticeable softening.

(2) After impact compression, the composite is structurally intact, demonstrating good plasticity when the strain rate is below 3000 s^{-1}. However, at the strain rate of 4500 s^{-1}, cracks develop along the edge of the sample, indicating a brittle cleavage fracture, as confirmed by the SEM image of the fracture.

(3) The damage mechanism of the graphene/aluminum composite is primarily governed by interfacial damage. This occurs because graphene does not deform under high-speed impact, leading to stress concentration around it. The stress experienced by the graphene is transmitted through the interface between the graphene and the matrix, resulting in damage to the matrix. As the strain rate increases, the stress range in the interface area expands, leading to significant plastic deformation of the matrix and further exacerbating interface damage.

(4) The comparison between the experimental results and the numerical simulation results reveals similar trends in mechanical changes. Although the numerical simulation results are slightly higher than the experimental results, the overall error remains below 10 %. This indicates a strong consistency between the two, demonstrating the effectiveness of the numerical simulation calculations.

Acknowledgment

This research was funded by the Future Industry Frontier Technology Project in Liaoning Province in 2025 (2025JH2/101330141) and Basic Research Projects

of Higher Education Institutions in Liaoning Province (JYTZD20230004).

6 REFERENCES

[1] H. Porwal, S. Grasso, M. J. Reece, Review of graphene–ceramic matrix composites, Advances in Applied Ceramics, 112 (**2013**) 8, 443–454, doi:10.1179/174367613X13764308970581

[2] T. K. Das, S. Prusty, Graphene-based polymer composites and their applications, Polymer-Plastics Technology and Engineering, 52 (**2013**) 4, 319–331, doi:10.1080/03602559.2012.751410

[3] S. C. Tjong, Recent progress in the development and properties of novel metal matrix nanocomposites reinforced with carbon nanotubes and graphene nanosheets, Materials Science and Engineering, 74 (**2013**) 10, 281–350, doi:10.1016/j.mser.2013.08.001

[4] Y. Li, X. M. Du, F. G. Liu, Study on microstructure and mechanical properties of graphene reinforced 6061 aluminum matrix composites, Journal of Shenyang Polytechnic University, 42 (**2023**) 2, 49–55, doi:10.3969/j.issn.1003-1251.2023.02.008

[5] Y. N. Shi, X. M. Du, F. G. Liu, Study on dynamic mechanical properties of graphene-reinforced aluminum matrix composites, Journal of Shenyang Polytechnic University, 41 (**2022**) 6, 74–79, doi:10.3969/j.issn.1003-1251.2002.06.012

[6] N. Li, X. M. Du, F. G. Liu, Effect of graphene copper plating on the structure and properties of aluminum matrix composites, Journal of Shenyang University of Technology, 40 (**2021**) 4, 73–77+87, doi:10.3969/j.issn.1003-1251.2021.04.013

[7] D. Fu, Y. Ling, P. Jiang, Y. Sun, C. Yuan, X. Du, Dynamic compressive properties of aluminium-matrix composites reinforced with SiC particles, Mater. Tehnol., 57 (**2023**) 2, 201–207, doi:10.17222/mit.2022.580

[8] M. Alteneiji, K. Krishnan, Z. W. Guan, W. J. Cantwell, Y. Zhao, G. Langdon, Dynamic response of aluminium matrix syntactic foams subjected to high strain-rate loadings, Composite Structures, 303 (**2023**), 116289, doi:10.1016/j.compstruct.2022.116289

[9] Z. Zaiemyekeh, G. H. Liaghat, H. Ahmadi, M. K. Khanc, O. Razmkhahc, Effect of strain rate on deformation behavior of aluminum matrix composites with Al_2O_3 nanoparticles, Materials Science and Engineering, 753 (**2019**), 276–284, doi:10.1016/J.MSEA.2019.03.052

[10] S. J. Niteesh Kumar, R. Keshavamurthy, M. R. Haseebuddin, P. G. Koppad, Mechanical properties of aluminium-graphene composite synthesized by powder metallurgy and hot extrusion, Transactions of the Indian Institute of Metals, 70 (**2017**), 605–613, doi:10.1007/s12666-017-1070-5

[11] M. Rashad, F. Pan, A. Tang, M. Asif, Effect of graphene nanoplatelets addition on mechanical properties of pure aluminum using a semi-powder method, Progress in Natural Science: Materials International, 24 (**2014**) 2, 101–108, doi:10.1016/j.pnsc.2014.03.012

[12] S. Zhao, S. Yan, X. Chen, Q. Hong, X. Li, S. Dai, Dynamic mechanical behavior of graphene nanoflakes reinforced aluminum matrix composites, Journal of Materials Engineering, 47 (**2019**) 3, 23–29, doi:10.11868/j.issn.1001–4381.2017.001177

[13] M. Dahiya, V. Khanna, S. A. Bansal, Aluminium-graphene metal matrix nanocomposites: Modelling, analysis, and simulation approach to estimate mechanical properties, Materials Today: Proceedings, 78 (**2023**), 414–419, doi:10.1016/j.matpr.2022.10.181

[14] M. Dahiya, V. Khanna, S. A. Bansal, Finite element analysis of the mechanical properties of graphene aluminium nanocomposite: varying weight fractions, sizes and orientation, Carbon Letters, (**2023**), 1–13, doi:10.1007/s42823-023-00543-x

[15] M. Dahiya, V. Khanna, S. A. Bansal, Effect of graphene size variation on mechanical properties of aluminium graphene nanocomposites: a modeling analysis, Materials Today: Proceedings, 73 (**2023**), 249–254, doi:10.1016/j.matpr.2022.07.259

[16] Y. Su, Z. Li, Y. Yu, Z. Li, Q. Guo, D. Xiong, D. Zhang, Composite structural modeling and tensile mechanical behavior of graphene reinforced metal matrix composites, Science China Materials, 61 (**2017**) 1, 112–124, doi:10.1007/s40843-017-9142-2

[17] E. D. H. Davies, S. C. Hunter, The dynamic compression testing of solids by the method of the split Hopkinson pressure bar, Journal of the Mechanics and Physics of Solids, 11 (**1963**) 3, 155–179, doi:10.1016/0022-5096(63)90050-4

[18] Y. Yuan, Y. Zhang, D. Ruan, A. Zhang, Y. Liang, P. J. Tan, P. Chen, Deformation and failure of additively manufactured Voronoi foams under dynamic compressive loadings, Engineering Structures, 284 (**2023**), 115954, doi:10.1016/j.engstruct.2023.115954

[19] Z. Zhang, T. Xu, W. Xin, J. Ding, N. Liu, Z. Wang, Y. Wang, X. C. Xia, Y. C. Liu, Compression performances of integral-forming aluminum foam sandwich, Composite Structures, 283 (**2022**), 115090, doi:10.1016/j.compstruct.2021.115090

[20] Y. F. Fan, Z. P. Duan, Experimental determination of Johnson-Cook material model parameters, Mechanics and Practice, 25 (**2023**) 5, 40–43, doi:10.3969/j.issn.1000-0879.2003.05.013

[21] Z. Jia, B. Guan, Y. Zang, Y. Wang, L. Mu, Modified Johnson-Cook model of aluminum alloy 6016-T6 sheets at low dynamic strain rates, Materials Science & Engineering A, 820 (**2021**), 141565, doi:10.1016/j.msea.2021.141565

[22] Y. F. Deng, Y. Zhang, H. P. Wu, X. Z. Zeng, Modification of Dynamic Mechanical Properties and J-C Constitutive Model of 6061-T651 Aluminum Alloy, Journal of Mechanical Engineering, 56 (**2019**) 20, doi:10.3901/JME.2020.20.074

[23] Y. K. Yang, B. Zhang, X. D. Wang, H. S. Zhang, Y. Wu, Y. J. Guan, Impact mechanical behavior of graphene and silicon carbide reinforced aluminum matrix composites, Journal of Materials Engineering, 47 (**2019**) 03, 15–22, doi:10.11868/j.issn.1001-4381.2017.001457

[24] X. Du, Z. Lu, S. Guo, Numerical simulation of dynamic mechanical properties of graphene-reinforced aluminum matrix composites, Mater. Tehnol., 56 (**2022**) 5, 499–506, doi:10.17222/mit.2022.477

[25] R. J. Arsenault, N. Shi, Dislocation generation due to differences between the coefficients of thermal expansion, Materials Science and Engineering, 81 (**1986**), 175–187, doi:10.1016/0025-5416(86)90261-2

[26] M. Rashad, F. Pan, A. Tang, M. Asif, Effect of graphene nanoplatelets addition on mechanical properties of pure aluminum using a semi-powder method, Progress in Natural Science: Materials International, 24 (**2014**) 2, 101–108, doi:10.1016/j.pnsc.2014.03.012

[27] T. Fiedler, M. Taherishargh, L. Krstulović-Opara, M. Vesenjak, Dynamic compressive loading of expanded perlite/aluminum syntactic foam, Materials Science and Engineering, 626 (**2015**), 296–304, doi:10.1016/j.msea.2014.12.032

[28] J. A. Sherwood, C. C. Frost, Constitutive modeling and simulation of energy absorbing polyurethane foam under impact loading, Polymer Engineering & Science, 32 (**1992**) 16, 1138–1146, doi:10.1002/pen.760321611